Thermal-Photon and Residual-Gas Scattering in the NLC Beam Delivery

I. Reichel, F. Zimmermann, P. Tenenbaum, T.O. Raubenheimer *
Stanford Linear Accelerator Center, Stanford University, California 94309

Abstract

Without collisions, the largest contribution to the beam lifetime in LEP is Compton scattering off thermal photons. Even if only a few particles are scattered in a single pass, the potential background generated could make this effect important for the NLC as well. We used a modified version of the tracking program DIMAD, which includes a Monte Carlo simulation for the Compton scattering on thermal photons, to calculate the fraction of scattered particles that are intercepted by downstream aperture restrictions and to determine the loss locations. We also studied particle losses due to other scattering processes. For all processes, the effect of additional collimators in the final focus was investigated.

1 INTRODUCTION

Without collisions, the largest contribution to the beam lifetime in LEP is Compton scattering off thermal photons. The effect was predicted by Telnov [1]. The backscattered photons were measured [2], they were observed also at HERA [3]. The beam lifetime measured at LEP is in good agreement with the simulated effect of scattering on thermal photons. The typical energy loss induced by this `inverse' Compton scattering increases in proportion to the beam energy. Even if only a few particles are scattered in a single pass, the potential background generated could make this effect important for the NLC. Assuming a typical photon energy, in the Zeroth Order Design Report (ZDR) [4] we estimated that about 36 particles per bunch train would scatter over a distance of 2 km, the length of the final focus. If this number is approximately correct, the Compton scattering on thermal photons could become a significant (and unavoidable) background source for the NLD detector.

We give the basic formulae describing the thermal-photon scattering and improve our previous crude estimate of the effect, by numerically integrating over the actual photon energy and angular distributions. We then use a version of the tracking program DIMAD [5], which was modified at CERN [6] and SLAC, and which includes a Monte Carlo simulation for the Compton scattering on thermal photons [7], to calculate the fraction of scattered particles that is lost and to determine the loss locations.

In Section 3, we employ the same version of DIMAD to study particle losses caused by two other scattering processes, namely by elastic and inelastic beam-gas scattering. Also here we discuss the total number of lost particles and their distribution. The effect of elastic scattering on atomic electrons is also estimated.

* Work supported by the U.S. Department of Energy under the contract DE-AC03-76SF00515.

2 SCATTERING ON THERMAL PHOTONS

The total cross section [1] for Compton scattering of a beam electron and a photon is

$$\sigma = \frac{2\pi r_e^2}{x}\left[\left(1-\frac{4}{x}-\frac{8}{x^2}\right)\ln(x+1) + \frac{1}{2}+\frac{8}{x}-\frac{1}{2(x+1)^2}\right] \quad (1)$$

$$\text{where} \qquad x = \frac{4E\omega_0\cos^2(\alpha/2)}{m^2c^4} \quad (2)$$

$$\approx 15.3\left[\frac{E}{\text{TeV}}\right]\left[\frac{\omega_0}{\text{eV}}\right]\cos^2(\alpha/2)$$

with α the incident photon angle with respect to the beam in the laboratory system, E the beam energy, and ω_0 the incident photon energy. For $x \ll 1$ the total cross section σ is roughly equal to the Thomson cross section $\sigma_0 = 8\pi r_e^2/3 = 6.65\times10^{-25}$ cm^2.

The energy spectrum of the scattered photons (and hence the energy loss of the electrons) is given by [1]

$$\frac{1}{\sigma}\frac{\mathrm{d}\sigma}{\mathrm{d}y} = \frac{2\sigma_0}{x\sigma}\left[\frac{1}{1-y}+1-y-4r(1-r)\right] \quad (3)$$

where $y=\omega'/E$ is the relative energy of the scattered photon, and $r = y/(x(1-y)) \le 1$.

The energy loss spectrum extends between 0 and a maximum value y_{max}

$$0 \le y \le y_{\max} = \frac{x}{1+x} \quad (4)$$

Only if x is sufficiently large can the scattered particles lose enough energy to hit some aperture. This becomes more likely the higher the beam energy and the higher the temperature of the vacuum chamber.

In Fig. 1 the total Compton scattering cross section and the maximum relative energy loss per scattering event are depicted as a function of the beam energy. In the following we always assume a beam energy of 500 GeV, unless noted otherwise.

The density and energy distribution of the thermal photons is given by the Planck formula:

$$\mathrm{d}n_\gamma = \frac{\omega_0^2\mathrm{d}\omega_0}{\pi^2c^3\hbar^3(e^{\omega_0/kT}-1)} \quad (5)$$

and the total number of photons per cm^3 is $n_\gamma \approx 20.2\ T^3$ cm^{-3} [1] with an average photon energy of $\bar{\omega}_0 = 2.7kT$. At 300 K, this is about 70 meV.

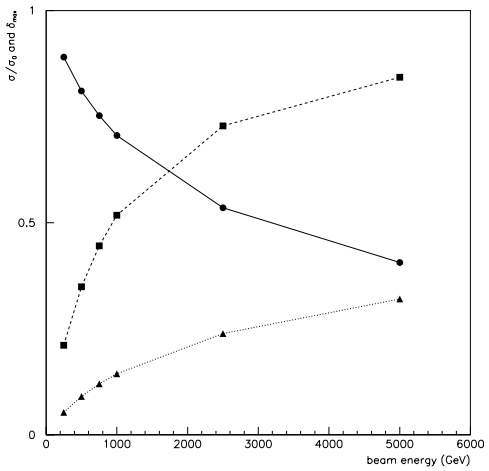

Figure 1: Total Compton cross section in units of the Thomson cross section (—, •) the maximum relative energy loss for head-on collision with a 0.07 eV thermal photon (- - -, squares), and the average relative energy loss ($\cdots$, triangles), all as a function of the beam energy. The total cross section and the average relative energy loss were obtained by a Monte-Carlo simulation generating 10^5 scattering events.

We consider a beam of N particles propagating through a distance L. The energy distribution of the scattered photons is obtained by integrating the product of cross section and Planck spectrum over the solid angle and over all photon energies [1]:

$$\frac{\mathrm{d}N}{\mathrm{d}y} = N L \int_0^{\pi} \int_{\omega_{min}}^{\infty} \frac{\mathrm{d}\sigma_c}{\mathrm{d}y} \, (1+\cos\alpha) \, \mathrm{d}n_\gamma(\omega_0, T) \, d\omega_0 \, \frac{\mathrm{d}\Omega}{4\pi} \quad (6)$$

where the factor $(1+\cos\alpha)$ accounts for the relative motion of electron and photon.

The minimum photon energy is a function of y,

$$\omega_{min} = \frac{y \, m_e^2 c^4}{4(1-y)E\cos^2\alpha/2} \quad (7)$$

and, to integrate Eq. (6), one must express x in terms of ω_0 and α using Eq. (3).

Figure 2 shows the energy loss spectrum, $\mathrm{d}N/\mathrm{d}y$ or $\mathrm{d}N/\mathrm{d}\delta$ (where $\delta = y$ is the relative energy loss of the electron), for $N = 10^{12}$ particles, a total length $L = 5$ km, and three different beam energies. By integrating $\mathrm{d}N/\mathrm{d}\delta$ over δ, we estimate a scattering probability of about $2.7 \times 10^{-14}\,\mathrm{m}^{-1}$ per particle, so that that about 100 particles will be scattered per bunch train. A significant fraction of these will suffer an energy loss large enough to hit some downstream aperture.

Figure 3 compares the energy-loss spectra for thermal-photon scattering with that for inelastic beam-gas scattering, assuming 10 nTorr of CO, both obtained from a Monte-Carlo simulation.

To gain more insight, we have performed simulations using a special version of DIMAD developed for LEP [6]: We tracked a few thousand particles through the NLC beam delivery system, with an optics as depicted in Figs. 4 and 5.

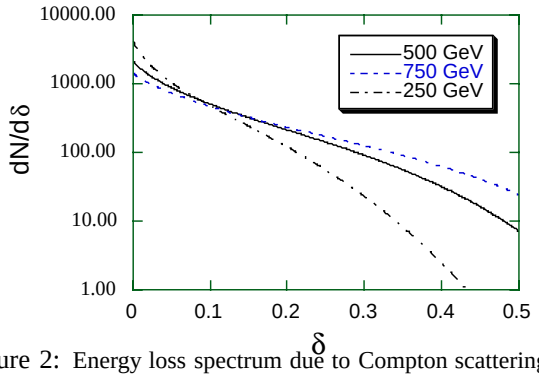

Figure 2: Energy loss spectrum due to Compton scattering off thermal photons The curves were obtained by numerical integration of Eq. (6). A beam pipe at room temperature was assumed.

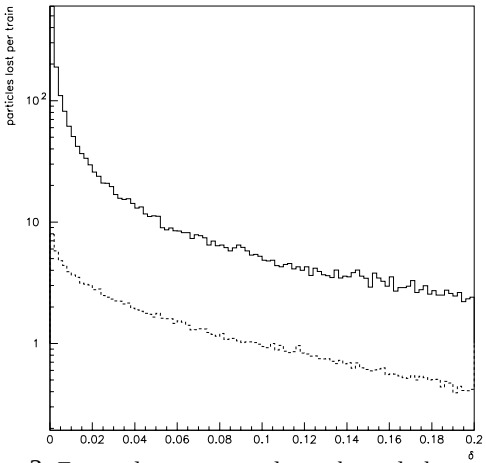

Figure 3: Energy-loss spectrum due to thermal-photon scattering (- - -) and inelastic beam-gas scattering (—).

The nominal number of NLC collimators was used : 4 horizontal plus 2 vertical spoilers, and 8 horizontal plus 6 vertical absorbers. They are adjusted to collimate at $5\,\sigma_x$, $36\,\sigma_y$, and 4 % in energy. Table 1 lists more details, including the locations of spoilers and absorbers in the collimation system (the first 2.5 km of the beam line). The collimation parameters chosen agree with the prescription of the ZDR. In order to explore the effect of additional collimation in the final focus proper, we consider 6 optional absorbers, two each for horizontal, vertical and energy collimation. Table 1 lists parameters of these final-focus collimators. Their locations are indicated in Figs. 4 and 5. For the three different scattering processes (thermal photon scattering, elastic and inleastic beam-gas scattering), we compare the particle losses obtained without any collimation in the final-focus, with all 6 final-focus collimators, and with only 4 transverse final-focus collimators.

The DIMAD simulations predict about 117 ± 2 scattering events per bunch train and 5 km distance. For 500 GeV beam energy, 51 ± 1 (44 %) of these particles are lost somewhere along the beam line. The loss distribution as a function of longitudinal position s is shown in Fig. 6. As can be seen by comparing with Fig. 5, most of the scattered particles are lost in the high dispersion regions of the collimation section and in the horizontal chromatic correction section (CCX) of the final focus. On average only

collimator type	coll. depth	half gap [mm]	location s [m]
collimators in the collimation system			
IP 1, hor. spoil. (Ti)	$5\,\sigma_x$, 4 %	2	383, 603
IP 1, vert. spoil. (Ti)	$36\,\sigma_y$	1.8	441
IP 1, hor. abs. (Cu)	$5\,\sigma_x$, 4 %	2	499, 719
IP 1, vert. abs. (Cu)	$36\,\sigma_y$	0.75	509
IP 1, vert. abs. (W)	$36\,\sigma_y$	1.8	661
FD 1, hor. spoil. (Ti)	$5\,\sigma_x$, 4 %	2	910, 1130
FD 1, vert. spoil. (Ti)	$36\,\sigma_y$	1.8	968
FD 1, hor. abs. (Cu)	$5\,\sigma_x$, 4 %	2	1026, 1246
FD 1, vert. abs. (Cu)	$36\,\sigma_y$	0.75	1036
FD 1, vert. abs. (W)	$36\,\sigma_y$	1.8	1188
IP 2, hor. abs. (W)	$15\,\sigma_x$	2.4	1431, 1652
IP 2, vert. abs. (Cu)	$150\,\sigma_y$	4.3	1490
FD 2, hor. abs. (W)	$6\,\sigma_x$	1.2	1967, 2187
IP 2, vert. abs. (Cu)	$40\,\sigma_y$	1.1	2025
optional collimators in the final focus			
hor. abs. at SX1 (2nd)	$6\,\sigma_x$	3.6	4097
hor. abs. at QY2 (2nd)	5 %	4.5	4630
vert. abs. at SY1 (2nd)	$45\,\sigma_y$	4.8	4715
hor. abs. at SI1	5 %	4.5	4798
hor. abs. at QFT6	$7\,\sigma_x$	3.3	5040
vert. abs. at QFT5	$50\,\sigma_y$	4.4	5056

Table 1: The collimators included in this study. The beam line starts with the post-linac diagnostic section at $s = 0$ m. The interaction point (IP) is at $s = 5210$ m. The labels 'IP' and 'FD' refer to collimators at the same betatron phase as the IP and the final doublet, respectively.

2 ± 0.3 particles are lost over the last 500 m, primarily in the quadrupole QFT6M (at 5041 m), and also near Q2M, the first quadrupole of the final doublet. At the latter place only about 0.2 ± 0.08 particles are lost per bunch train. These particle numbers do not change dramatically with beam energy: at 250 GeV about 40 ± 1 particles are lost per train, and at 750 GeV the number is 56 ± 1.

The simulations are performed with a version of DIMAD which correctly treats the transverse dynamics even for large energy deviations. Figure 7 presents a result that was obtained for identical conditions with the original DIMAD program that is accurate only to 2nd order in δ. The difference between Figs. 6 and 7 is small.

Figure 8 presents the results of simulations including 6 or 4 final-focus collimators, shown in the left and right picture, respectively. In these two cases, about 66 % of the scattered particles are lost, compared with 44 % in the absence of final-focus collimation. But now, there are no particles lost near the final doublet, whereas without final-focus collimation the loss there was about 0.2 per train. This suggests that the additional final-focus collimators would be effective.

3 BEAM-GAS SCATTERING

3.1 Elastic Scattering

The cross section for elastic scattering (Mott scattering) is given by [6]

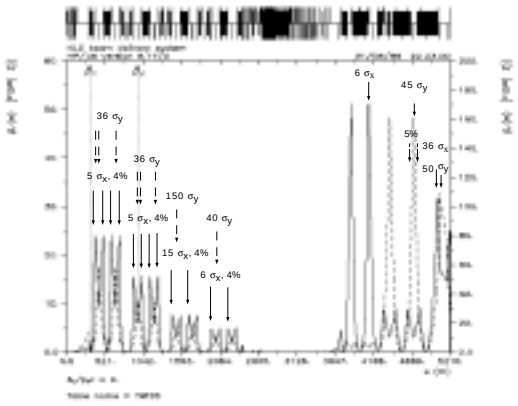

Figure 4: Horizontal and vertical beta functions in the NLC beam delivery system. The locations of spoilers and absorbers in the collimation system (the first 2.5 km) and possible locations in the final focus proper (the last 1.8 km) are also indicated, along with the respective collimation depths.

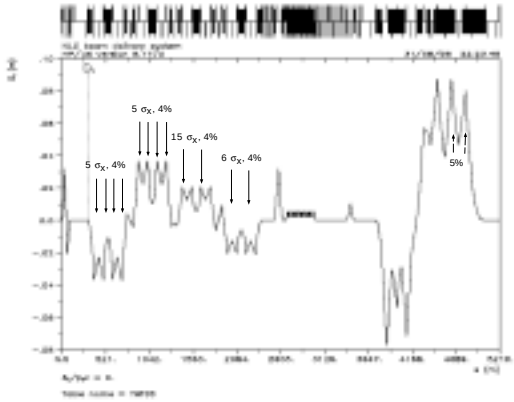

Figure 5: Dispersion function in the NLC beam delivery system. The locations of spoilers and absorbers for energy collimation are marked as in Fig. 4.

$$\frac{\mathrm{d}\sigma_{el}}{\mathrm{d}\Omega} = \left(\frac{Z\alpha\hbar c}{2pv}\right)^2 \frac{1-\beta^2\sin^2\theta/2}{\sin^4\theta/2} \tag{8}$$

Integrated above some minimum angle θ_{min} the total cross section is approximately

$$\sigma_{el} \approx \frac{\pi\alpha^2\hbar^2c^2Z^2}{E^2\sin^2\theta/2}. \tag{9}$$

A minimum angle determined by the screening due to the atomic electrons is given by $\theta_{min} \approx \hbar/(pa) \approx 20$ nrad, with $a \approx 0.22\lambda\!\!\!^{-}_c/\alpha Z^{1/3}$ and assuming $Z \approx 7$ (nitrogen, or carbon monoxide molecules)[1]. The total cross section is then $\sigma_{el} \approx 10^{-23}$ m^{-2}. At a CO pressure of 10 nTorr, this translates into a scattering probability of 8×10^{-9} m^{-1}, or 4×10^7 scatters per bunch train. The simulations show that the particles scattered at angles below 1 μrad are not lost. Instead of 20 nrad, we thus assumed a limit $\theta_{min} = 2\,\mu$rad, for which the scattering probability is 8×10^{-13} m^{-1}, resulting in about 4000 scattering events per train. About 30 % of these lead to a particle loss (1000 particles per

[1]The minimum beam divergence at the high beta points is much smaller than this, only about 0.5 nrad.

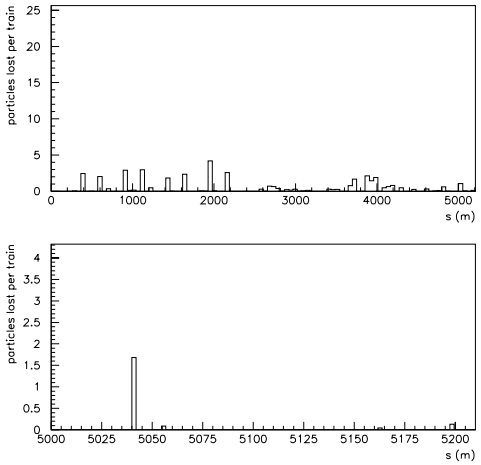

Figure 6: Number of particles per bunch train lost due to thermal-photon scattering at different locations along along the beam line. Top: the entire beam-delivery system, bottom: the last 200 m prior to the IP.

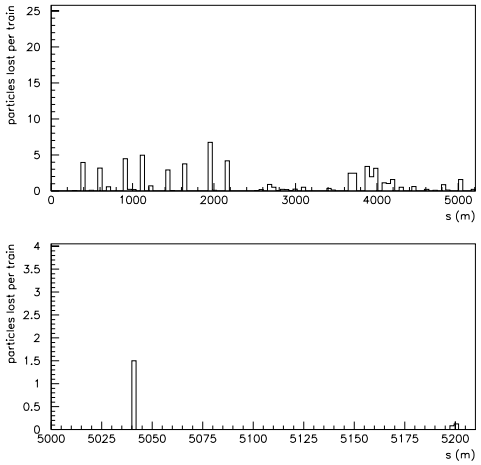

Figure 7: Same figure as Fig. 6 but calculated with the original DIMAD program. The latter is chromatically correct only to 2nd order in δ.

train in the entire 5 km beam-delivery section). The loss distribution is illustrated in Fig. 9. Most losses occur at the spoilers and absorbers of the collimation section.

In Fig. 10 we depict simulation results obtained including final-focus collimators. With or without these collimators, there are no losses in the immediate vicinity of the final doublet. The losses 150–200 m upstream of the final doublet are reduced by the additional collimation. The fraction of scattered particles (at an angle larger than 2 μrad) which are lost is about 43 %, a factor of 1.5 higher than without final-focus collimation.

3.2 Inelastic Scattering

The differential cross section for inelastic scattering (Bremsstrahlung) is approximately given by

$$\frac{\mathrm{d}\sigma}{\mathrm{d}\delta} = \frac{A}{N_A X_0}\,\frac{1}{k}\,\left(\frac{4}{3} - \frac{4}{3}k + k^2\right) \qquad (10)$$

where N_A is the Avogadro number, A the atomic mass, and

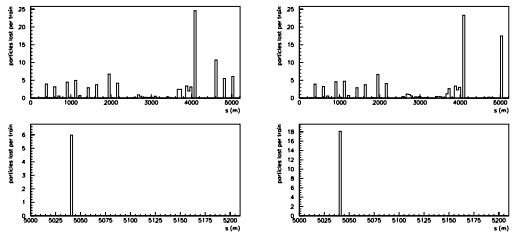

Figure 8: Number of particles per bunch train lost due to thermal-photon scattering at different locations along along the beam line. Left: with 6 additional final-focus collimators; right: with 4 final-focus collimators.

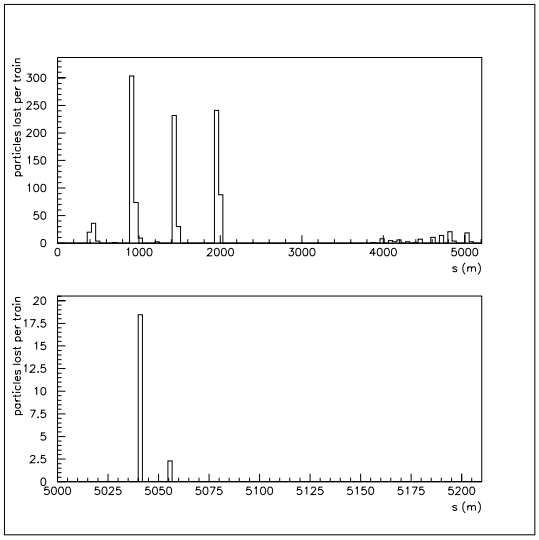

Figure 9: Number of particles per bunch train lost due to elastic beam-gas scattering at different locations along the beam line, without final-focus collimation.

$$\frac{1}{X_0} \approx 4\alpha r_e^2 N_A\,\frac{Z^2}{A}\,\ln\left(\frac{183}{Z^{1/3}}\right) \qquad (11)$$

the radiation length. The total cross section for scattering with a relative energy loss larger than δ_{min} is given by [8]

$$\sigma_{inel} \approx -\frac{16}{3} r_e^2 \alpha Z^2 \ln\delta_{min}\,\ln\left(\frac{183}{Z^{1/3}}\right) \qquad (12)$$

For $\delta_{min} = 1\,\%$ and CO or N_2 molecules, this cross section is about 6 barn. At a pressure of 10 nTorr, the scattering probability is $2 \times 10^{-13}\,\mathrm{m}^{-1}$. This corresponds to 1000 events per bunch train over 5 km. About half of these (500 per train) are lost by hitting aperture or collimators,

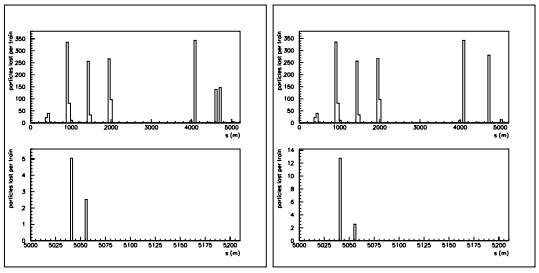

Figure 10: Number of particles per bunch train lost due to elastic beam-gas scattering at different locations along the beam line. Left: with 6 additional final-focus collimators; right: with 4 final-focus collimators.

and almost 20 ± 3 hit apertures within 200 m from the IP. The simulated loss distribution is shown in Fig. 11.

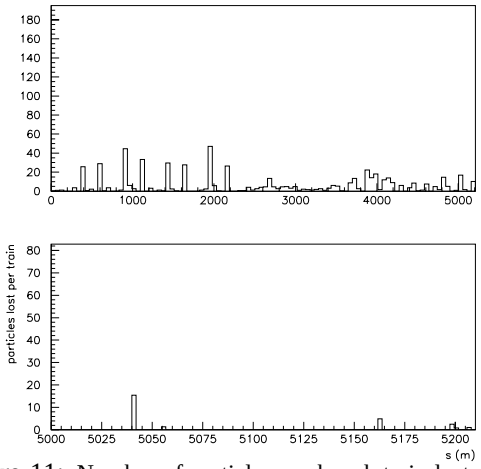

Figure 11: Number of particles per bunch train lost due to inelastic beam-gas scattering at different locations along the beam line, without final-focus collimation.

Figure 12 again shows the effect of final-focus collimators. Also in this case, considerably more scattered particles are lost in the final focus than would be without final-focus collimation. In total, about 80 % of the particles scattered with an energy loss above 1 % are lost. Without final-focus collimation this fraction was 58 %. The final-focus collimators do however reduce the number of particles lost within 50 m from the final doublet by roughly a factor of 2, from about 10 to about 5 (note the different scale of the two bottom pictures).

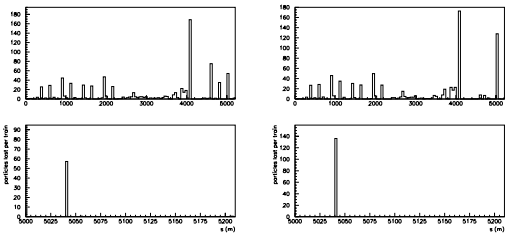

Figure 12: Number of particles per bunch train lost due to inelastic beam-gas scattering at different locations along the beam line. Left: with 6 additional final-focus collimators; right: with 4 final-focus collimators.

3.3 Scattering on Atomic Electrons

If an electron scatters elastically on an atomic electron, in the laboratory frame it can lose a significant fration of its energy. The cross section for scattering on atomic electrons is

$$\frac{\mathrm{d}\sigma}{\mathrm{d}\delta} = -\frac{2\pi r_e^2 n_{atom} Z}{\gamma} \left\{ \frac{1 - 2\delta + 3\delta^2 - 2\delta^3 + \delta^4}{\delta^2 (1 - 2\delta + \delta^2)} \right\} \approx -\frac{2\pi r_e^2 n_{atom} Z}{\gamma \delta^2} \quad (13)$$

where Z is the atomic number of the residual gas atoms, n_a the number of atoms per molecule, r_e the classical electron radius and $\delta > 0$. Integration yields the total cross section for losing an energy larger than δ_{min}: $\sigma = 2\pi r_e^2 Z)/\gamma\delta_{min})$. For example, with $Z = 8$ and $\delta_{min} = 1\,\%$, the cross section is $\sigma = 8 \times 10^{-28}\,\mathrm{cm}^2$. This would amount to only 0.1 scattered particles per bunch train, a negligible effect. The energy loss δ and the scattering angle in the center-of-mass frame are related by $\delta = (\cos\theta^* - 1)/2$. The scattering angle in the laboratory frame is

$$\tan\theta = \frac{1}{\sqrt{2\gamma}} \frac{2\sqrt{\delta + \delta^2}}{1 - 2\delta} \quad (14)$$

As an example, for $\delta \approx 0.1\,\%$ the scattering angle would be $\theta \approx 44\,\mu$rad.

4 CONCLUSIONS

In the 5 km long NLC beam delivery system, about one thousand particles per train are lost due to elastic beam-gas scattering and about five hundred due to inelastic beam-gas scattering (Bremsstrahlung), assuming 10 nTorr average CO pressure. Of these particles, only about 10 and 20, respectively, are lost over the last 200 m prior to the IP. These are 10 times more than the number of particles lost by scattering on thermal photons, which are about 50 in total, and 2 over the last 200 m. At a vacuum pressure of about 1 nTorr, the losses due to beam-gas scattering and due to thermal-photon scattering would be equal.

5 ACKNOWLEDGEMENTS

We thank our colleagues at CERN, in particular Helmut Burkhardt and Ghislain Roy, who helped writing the modified version of DIMAD used for these studies.

6 REFERENCES

[1] V.I. Telnov, “Scattering of Electrons on Thermal Radiation Photons in Electron-Positron Storage Rings”, Nucl. Instr. Methods A, p. 304 (1987).

[2] B. Dehning et al., “Scattering of high energy electrons off thermal photons”, Phys. Lett. B249 p. 145 (1990).

[3] M. Lomperski, “Compton Scattering off Blackbody Radiation and other Backgrounds of the HERA Polarimeter”, DESY-93-045 (1993).

[4] C. Adolphsen et al., “Zeroth Order Design Report for the Next Linear Collider,” *SLAC-Report* **474** (1996).

[5] R.V. Servranckx, K.L. Brown, L. Schachinger, D. Douglas, “User's Guide to the Program DIMAD”, SLAC-285 (1990).

[6] I. Reichel, “Study of the Transverse Beam Tails at LEP”, Ph.D. thesis, RWTH Aachen (1998).

[7] H. Burkhardt, “Monte Carlo Simulations of Scattering of Beam Particles and Thermal Photons”, CERN SL/Note 93-73 (OP) (1993).

[8] A. Piwinski, “Beam Losses and Lifetime”, in CERN Accelerator School, Gif-sur-Yvette, France, CERN 85-19 Vol. II (1985).